Journal of Sound and Vibration (1999) **227**(4), 769–785
Article No. jsvi.1999.2384, available online at http://www.idealibrary.com on IDEAL

DYNAMIC ANALYSIS OF MULTI-STEPPED, DISTRIBUTED PARAMETER ROTOR-BEARING SYSTEMS

S.-W. HONG AND J.-H. PARK

School of Mechanical Engineering, Kumoh National University of Technology, 188 Shinpyung, Kumi, Kyungbuk 730-701, *Korea*

(*Received* 29 *October* 1998, *and in final form* 11 *May* 1999)

Exact solutions for a distributed parameter system are of great use for the physical understanding of the system or the sensitivity analysis and design of the system. However, exact or closed-form solutions for multi-stepped rotor-bearing systems with distributed parameters have been rarely investigated. The present paper proposes a modelling and analysis method to obtain exact solutions for multi-stepped rotor-bearing systems with distributed parameters. To this end, a modelling procedure to obtain an exact dynamic matrix for a Timoshenko shaft element is presented by using a spatial state equation and the Laplace transformation. The assembling procedure for constructing the global matrix can be accomplished in the same manner as the finite element method. The proposed method can readily provide exact eigensolutions, frequency responses and unbalance responses for multi-stepped rotor-bearing systems with distributed parameters. Three numerical examples are also presented for validating or illustrating the proposed method. The numerical study shows that the proposed method is very useful for the analysis of rotor-bearing systems.

1. INTRODUCTION

Although the dynamics for rotor-bearing systems can be well represented by a partial-differential equation of time and axial co-ordinate as already available in the literature, it does not seem to be easy enough to solve the equation or account for complex shape and boundary conditions of actual systems. Consequently, dynamic analysis for a complicated system relies solely on a numerical procedure dealing with matrices that are acquired through discretization of distributed-parameter system equations into approximate, finite degree-of-freedom (d.o.f.) system equations. Among discretization methods available for rotor-bearing systems, the transfer matrix method (TMM) [1–4] and the finite element method (FEM) [5–9] have been preferably employed. Especially, the FEM has been an indispensable tool by virtue of remarkable advance in computer technology. However, there still remains the problem of quantifying the errors associated with discretization. On the other hand, exact solutions for a structural dynamic system are of great use for the physical understanding of the system or the sensitivity analysis and design of the system. Many researchers have studied the rotor

0022-460X/99/440769 + 17 $30.00/0

dynamics with the analysis of a simple, distributed-parameter rotor system in order to understand fundamental features of rotating machinery [10–13]. However, exact or closed-form solutions for multi-stepped rotor-bearing systems with distributed parameters have been rarely investigated.

Recently, Yang and Fang [14, 15] presented an interesting method to obtain exact and closed solutions for distributed parameter rotor-bearing systems by using the distributed transfer function synthesis (DTFS) technique. The concept and derivation procedure of the DTFS is believed to be useful for the modelling and analysis of distributed parameter rotor-bearing system. However, the resultants for rotor-bearing systems seem to be very complicated because they include 8×8 distributed transfer function matrices that should be integrated over the length of the shaft element. In this paper, an improved modelling method is suggested that can provide exact and closed form solutions for multi-stepped, distributed-parameter rotor-bearing systems. A comprehensive modelling procedure to obtain an exact dynamic matrix for a uniform Timoshenko shaft element is presented. First, a spatial state equation is constructed for a Timoshenko shaft model, which contains gyroscopic moment, rotary inertia and shear deformation. Second, Laplace transformation is applied to the state equation with respect to time. Then the state equation is Laplace transformed once more with respect to the spatial co-ordinate. Inverse Laplace transformation, after resolving the inverse matrix formula, for the resulting equation with respect to the spatial co-ordinate, leads to an exact transfer matrix between the boundary values at one end and the values at an in-between point of a shaft element. Substitution of the other boundary values for the shaft element into the resulting equation and rearrangement of the variables yields an element dynamic matrix, which can be thought of as an exact dynamic element matrix for a uniform Timoshenko shaft element. In particular, the use of complex co-ordinates in the formulation makes it convenient to derive the exact dynamic element matrix for the shaft element. Laplace domain equations for the other two essential elements, i.e., bearing and rigid disk elements are also derived. The assembling procedure for constructing the global matrix can be easily accomplished in the same manner that the global mass and stiffness matrices are constructed in FEM. The complex conjugate equation of motion for the uniform Timoshenko shaft element is also constructed and assembled simultaneously to take into account the anisotropy in the system. The proposed method can readily provide exact eigensolutions, frequency responses and unbalance responses for distributed-parameter rotor-bearing systems.

The proposed method has several advantages. The most important feature of the method is that the method can deliver exact and closed-form dynamic solutions for multi-stepped, distributed parameter rotor-bearing systems. A great reduction for the system matrix size is also expected due to the facts that a uniform shaft segment, regardless of the length, can be modelled by an element and that most rotating machinery are composed of a few uniform shaft segments. The parametric study with changing parameters for any uniform shaft section can be easily accomplished through the proposed method, different than the FEM, which requires re-meshing to adjust properties of every element relevant to the parameters. Three numerical examples are provided. In the first example, the proposed method is compared with

the FEM from reference [7]. In the second example, a two-stepped rotor-bearing system problem is considered to illustrate the advantage of the proposed method in design. In the final example, the proposed method is applied to a general, multi-stepped rotor-bearing system to show the applicability of the method. The numerical study shows that the proposed method is very useful for the dynamic analysis or design of rotor-bearing systems.

2. MODELLING

2.1. MODELLING OF TIMOSHENKO SHAFT ELEMENT

A Timoshenko shaft model is shown in Figure 1. The equations of motion for the Timoshenko shaft, which contains gyroscopic moment, shear deformation and rotary inertia, can be written in complex co-ordinates as

$$f = kAG\left(\phi - \frac{\partial p}{\partial x}\right),$$

$$m = EI_d \frac{\partial \phi}{\partial x},$$

$$\frac{\partial f}{\partial x} = -\rho A \frac{\partial^2 p}{\partial t^2},$$

$$\frac{\partial m}{\partial x} - f = \rho I_d \frac{\partial^2 \phi}{\partial t^2} - \mathrm{j}\Omega \rho I_p \frac{\partial \phi}{\partial t}, \tag{1}$$

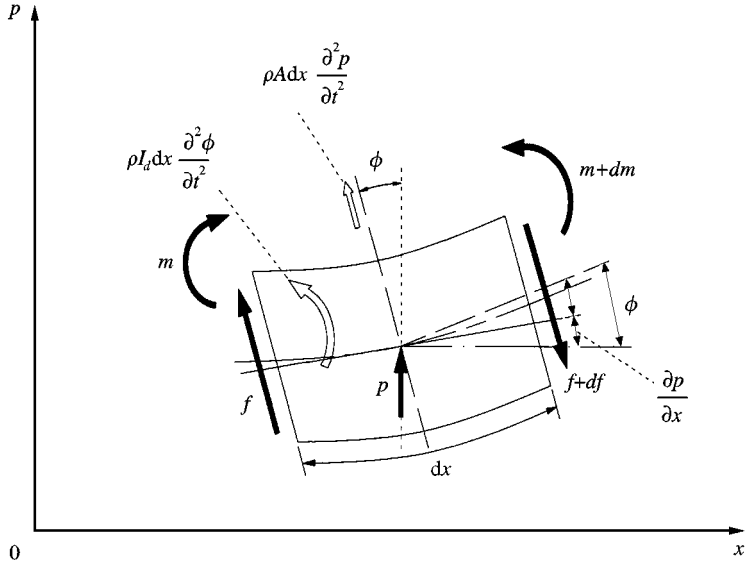

Figure 1. Timoshenko shaft.

where p and ϕ are the complex, transverse and angular displacements respectively, defined as

$$p = y + \mathrm{j}z, \quad \phi = \theta_y + \mathrm{j}\theta_z.$$

In addition, f and m are the complex shear force and moment respectively, defined as

$$f = f_y + \mathrm{j}f_z, \quad m = m_y + \mathrm{j}m_z.$$

ρ, G and E are the density, shear modulus and Young's modulus respectively. A, I_d and I_p are the area, diametral and polar area moments of inertia respectively, and k is the shape factor that is dependent on the cross-sectional shape (for example, 9/10 for circular cross-section). Ω is the rotational speed.

Equation (1) can be rewritten, in a state-space form for the spatial co-ordinate x, as

$$\frac{\partial p}{\partial x} = \phi - \frac{f}{kAG}, \qquad \frac{\partial \phi}{\partial x} = \frac{m}{EI_d}, \qquad \frac{\partial f}{\partial x} = -\rho A \frac{\partial^2 p}{\partial t^2},$$

$$\frac{\partial m}{\partial x} = f + \rho I_d \frac{\partial^2 \phi}{\partial t^2} - \mathrm{j}\Omega \rho I_p \frac{\partial \phi}{\partial t}. \tag{2}$$

Laplace transformation of equation (2) with respect to time, with zero initial conditions, leads to

$$\frac{\partial P}{\partial x} = \Phi - \frac{F}{kAG}, \qquad \frac{\partial \Phi}{\partial x} = \frac{M}{EI_d}, \qquad \frac{\partial F}{\partial x} = -\rho A s^2 P,$$

$$\frac{\partial M}{\partial x} = F + \rho I_d s^2 \Phi - \mathrm{j}\Omega \rho I_d s \Phi. \tag{3}$$

Here, s is the Laplace variable for time and the capital letters, i.e., P, Φ, F and M denote Laplace transforms for the corresponding lower-case letters. Equation (3) can be represented, in a simple matrix form, as follows:

$$\frac{\partial \Psi(x, s)}{\partial x} = B(s)\Psi(x, s), \tag{4}$$

where

$$\Psi(x, s) = \begin{Bmatrix} P \\ \Psi \\ F \\ M \end{Bmatrix}, \qquad B(s) = \begin{bmatrix} 0 & 1 & -d & 0 \\ 0 & 0 & 0 & b \\ -c & 0 & 0 & 0 \\ 0 & a & 1 & 0 \end{bmatrix}.$$

Here

$$a = \rho I_d s^2 - \mathrm{j}\Omega\rho I_p s, \qquad b = \frac{1}{EI_d}, \quad c = \rho A s^2, \quad d = \frac{1}{kAG}.$$

Laplace transformation of equation (4) for the spatial co-ordinate x with consideration of boundary values at $x = 0$ may yield

$$\tilde{\Psi}(\lambda, s) = [\lambda I - B]^{-1}\Psi(0, s). \tag{5}$$

Here, λ is the Laplace variable for the spatial co-ordinate and $\tilde{\Psi}(\lambda, s)$ represents the Laplace transform for $\Psi(x, \lambda)$. One can resolve $[\lambda I - B]^{-1}$ in equation (5) to obtain each element as shown in Appendix A.

With the help of equations (A1) and (A2) in Appendix A inverse Laplace transformation of equation (5) for x gives the following:

$$\Psi(x, s) = C(x, s)\Psi(0, s), \tag{6}$$

where $C(x, s)$ is given in equation (A3). Here, consider a uniform shaft element as shown in Figure 2. In addition, let us make use of the sign conventions as indicated in Figure 2 for the nodal values of the elements at $x = 0$ and l. Substitution of the nodal values into equation (6) and rearrangement of the variables in equation (6) yield

$$\begin{Bmatrix} F_1 \\ M_1 \\ F_2 \\ M_2 \end{Bmatrix} = d^s \begin{Bmatrix} P_1 \\ \Phi_1 \\ P_2 \\ \Phi_2 \end{Bmatrix}, \tag{7}$$

where

$$d^s = \frac{\alpha^2 - \beta^2}{\Delta} \begin{bmatrix} d_1 & d_2 & d_4 & d_5 \\ d_2 & d_3 & -d_5 & d_6 \\ d_4 & -d_5 & d_1 & -d_2 \\ d_5 & d_6 & -d_2 & d_3 \end{bmatrix} \tag{8}$$

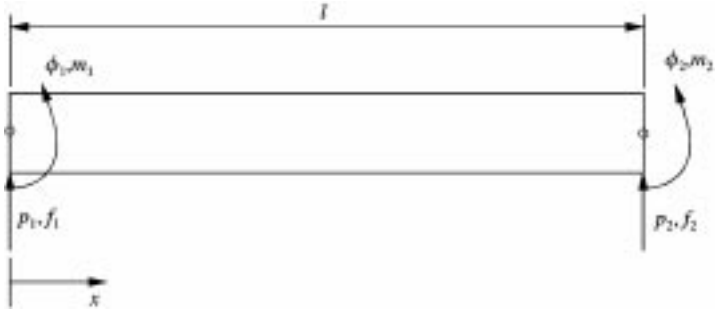

Figure 2. A uniform shaft element and the sign conventions for the nodal values.

and Δ, d_i, $i = 1, 2, \ldots, 6$ are presented in equation (A5). Equation (8) is the element dynamic matrix in the s domain, which represents an exact relationship between nodal forces and nodal displacements for the shaft element. As shown in equation (8), mass and stiffness matrices cannot be explicitly separated out of the exact dynamic element matrix. Conventional discretization methods such as FEM and TMM give mass and stiffness matrices, which eventually result in approximated second order polynomials of s. Equation (7) appears to have finite d.o.f.s. However, the transcendental functions in equation (8) can be rewritten as infinite order polynomials of s, implying that the system still retains a nature of infinite d.o.f.s system.

For taking account of the anisotropy in rotor-bearing systems, there is a need to deal with the complex conjugate partial differential equations. For the complex conjugate partial differential equations of motion, the parameters in equation (4) should be replaced as follows:

$$\hat{a} = \rho I_d s^2 + \mathrm{j}\Omega\rho I_p s, \quad \hat{b} = b = \frac{1}{EI_d}, \quad \hat{c} = c = \rho A s^2, \quad \hat{d} = d = \frac{1}{kAG},$$

where the $\hat{}$ denotes the parameters for the conjugate equations. Then, the conjugate element dynamic equation can be written as

$$\begin{Bmatrix} \hat{F}_1 \\ \hat{M}_1 \\ \hat{F}_2 \\ \hat{M}_2 \end{Bmatrix} = \hat{d}^s \begin{Bmatrix} \hat{P}_1 \\ \hat{\Phi}_1 \\ \hat{P}_2 \\ \hat{\Phi}_2 \end{Bmatrix}, \tag{9}$$

where

$$\hat{d}^s = \frac{\hat{\alpha}^2 - \hat{\beta}^2}{\Delta} \begin{bmatrix} \hat{d}_1 & \hat{d}_2 & \hat{d}_4 & \hat{d}_5 \\ \hat{d}_2 & \hat{d}_3 & -\hat{d}_5 & \hat{d}_6 \\ \hat{d}_4 & -\hat{d}_5 & \hat{d}_1 & -\hat{d}_2 \\ \hat{d}_5 & \hat{d}_6 & -\hat{d}_2 & \hat{d}_3 \end{bmatrix} \tag{10}$$

and $\hat{\alpha}^2$, $\hat{\beta}^2$, $\hat{\Delta}$, and $\hat{d}_i$, $i = 1, 2, \ldots, 6$, are given in equations (A6) and (A7). The hat $\hat{}$ for the variables in equation (9) denotes Laplace transforms for the corresponding variables. It should be noted here that the Laplace transform for the complex conjugate of a complex variable does not necessarily be complex conjugate of the Laplace transform for the complex variable.

2.2. MODELLING OF DISK ELEMENT

The equations of motion for a rigid disk and the conjugate equations can be written as

$$m^d \ddot{p} = f, \quad J_d^d \ddot{\phi} - \mathrm{j}\Omega J_d^d \dot{\phi} = m, \tag{11a}$$

$$m^d \ddot{\bar{p}} = \bar{f}, \quad J_d^d \ddot{\bar{\phi}} + \mathrm{j}\Omega J^d \dot{\bar{\phi}} = \bar{m}, \tag{11b}$$

where $(-)$ denotes the complex conjugate. Applying Laplace transformation to equations (11a) and (11b) provides the following equation of motion, in the s domain, for the disk element

$$\begin{Bmatrix} F \\ M \end{Bmatrix} = d^d \begin{Bmatrix} P \\ \Phi \end{Bmatrix}, \quad \begin{Bmatrix} \hat{F} \\ \hat{M} \end{Bmatrix} = \hat{d}^d \begin{Bmatrix} \hat{P} \\ \hat{\Phi} \end{Bmatrix}, \tag{12}$$

where

$$d^d = \begin{bmatrix} m_d s^2 & 0 \\ 0 & J_d s^2 - \mathrm{j}\Omega J_p s \end{bmatrix}, \quad \hat{d}^d = \begin{bmatrix} m_d s^2 & 0 \\ 0 & J_d s^2 + \mathrm{j}\Omega J_p s \end{bmatrix}.$$

2.3. MODELLING OF BEARING ELEMENT

The equation of motion for a bearing element and the conjugate equation can be written as

$$f = c_f \dot{p} + c_b \dot{\bar{p}} + k_f p + k_b \bar{p},$$

$$\bar{f} = \bar{c}_f \dot{\bar{p}} + \bar{c}_b \dot{p} + \bar{k}_f \bar{p} + \bar{k}_b p. \tag{13}$$

The complex stiffness and damping coefficients of bearing element are defined as [13]

$$2c_f = c_{yy} + c_{zz} - \mathrm{j}(c_{yz} - c_{zy}), \quad 2c_b = c_{yy} - c_{zz} + j(c_{yz} + c_{zy}),$$

$$2k_f = k_{yy} + k_{zz} - \mathrm{j}(k_{yz} - k_{zy}), \quad 2k_b = k_{yy} - k_{zz} + j(k_{yz} + k_{zy}).$$

The Laplace transformation for equation (13) with respect to time leads to

$$\begin{Bmatrix} F \\ \hat{F} \end{Bmatrix} = \begin{bmatrix} d_f^b & d_b^b \\ \hat{d}_b^b & \hat{d}_f^b \end{bmatrix} \begin{Bmatrix} P \\ \hat{P} \end{Bmatrix}, \tag{14}$$

where

$$d_f^b = c_f s + k_f, \quad d_b^b = c_b s + k_b, \quad \hat{d}_f^b = \bar{c}_f s + \bar{k}_f \quad \hat{d}_b^b = \bar{c}_b s + \bar{k}_b.$$

2.4. ASSEMBLING PROCEDURE FOR THE GLOBAL SYSTEM DYNAMIC MATRIX

The assembling procedure for the global system dynamic matrix can be summarized as follows: first, decompose the rotor shaft system into uniform, distributed parameter shaft elements and discrete disk or bearing elements. Second, make an element dynamic matrix for each of the shaft, disk and bearing elements with equations (7), (9), (12) and (14). Third, assemble the element dynamic matrices

in the same manner that the global matrices are constructed in FEM. This procedure may result in the following system matrix equation:

$$\begin{Bmatrix} F \\ \hat{F} \end{Bmatrix} = D(s) \begin{Bmatrix} Q \\ \hat{Q} \end{Bmatrix}, \tag{15}$$

where Q and $\hat{Q}$ are Laplace transforms of the global displacement vector and the complex conjugate vector respectively, and F and $\hat{F}$ are Laplace transforms of the corresponding force vectors:

$$D(s) = \begin{bmatrix} D^s + D^d + D_f^b & D_b^b \\ \hat{D}_b^b & \hat{D}^s + \hat{D}^d + \hat{D}_f^b \end{bmatrix}$$

and the subsidiary system dynamic matrices, D^i, $\hat{D}$, $i = s, d, b$, are assembled matrices associated with shaft, disk and bearing, respectively. The transfer function matrix is defined by the inverse of $D(s)$ and, in consequence, the frequency response function matrix might be computed as

$$H(\mathrm{j}\omega) = \{D(\mathrm{j}\omega)\}^{-1}, \tag{16}$$

where ω is the excitation frequency. From equation (15), the eigenvalue problem is defined as

$$D(s)U = 0. \tag{17}$$

Eigenvalues can be determined by finding roots that satisfy $\det\{D(s)\} = 0$. Once the eigenvalues are determined, the corresponding eigenvectors may be easily determined by substituting the eigenvalues into equation (17). On the other hand, the time response cannot be calculated directly but must be calculated indirectly by applying the convolution integral with impulse response functions attained through inverse Fourier transformation of the frequency response functions.

3. NUMERICAL ANALYSIS AND DISCUSSION

Three examples are taken to show the adequacy and applicability of the proposed method. In the first example, the proposed method is compared with FEM to validate the proposed method. In the second example, a parametric study for the effect of shaft length variation of a rotor system that consists of two shafts with different diameters is demonstrated to show the usefulness of the method in design. In the final example, an unbalance response analysis is performed to show the applicability of the proposed method for a more complicated multi-stepped rotor system.

3.1. NUMERICAL EXAMPLE 1

In Figure 3 is shown the numerical model, which is composed of a uniform shaft of 1·2 m and 2·5 cm respectively, in length and diameter, and two identical bearings

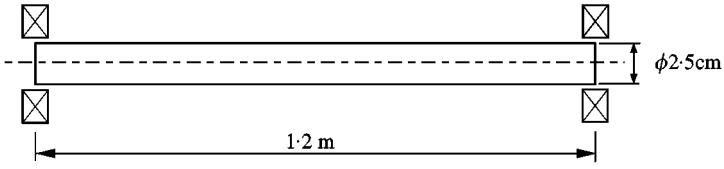

Figure 3. Numerical model 1.

at both ends of the shaft. The bearing stiffness and damping coefficients are $k_f = 12 \times 10^5$ N/m, $k_b = 0$, $c_f = 6$ Ns/m, and $c_b = 0$. In this example, the proposed method is compared with the FEM from reference [7]. The finite element model in this case also includes gyroscopic effect, rotary inertia and shear deformation. In the proposed method, only one element is taken to model the shaft, while in the FEM, several different numbers of elements are taken to notice the difference. Frequency response functions (FRFs) by the proposed method and the FEM are compared in Figure 4. The FEM always generates peak frequencies (natural frequencies) located higher than those from the proposed method. In particular, these peak frequencies converge to the peak frequencies from the proposed method as the number of elements is increased. This implies that the proposed method provides exact solutions. Eigenvalues computed from the proposed method and the FEM are also compared in Table 1. From Figure 4 and Table 1, it can be concluded that a uniform shaft can be modelled by one exact element matrix proposed in this paper without causing any error.

3.2. NUMERICAL EXAMPLE 2

In this example, a simple parametric study for a shaft-disk-bearing system is performed so as to show that the proposed method is very useful for changing the dimensions or properties of an element. Due to the fact that a uniform shaft section can be modelled with only one element regardless of the size of the element, the proposed method allows object-oriented programming. The schematic drawing for the rotor-bearing system considered in this example is shown in Figure 5. The detailed specifications of the rotor-bearing system are given in Table 2. The rotational speed of the rotor is set to 6000 r.p.m. Two shaft elements are used for modelling.

In Figure 6 is shown a typical FRF for the system with $L_1/L_2 = 1{\cdot}0$ when measured and excited at the left and right bearing positions respectively. First forward and backward natural frequencies with changing the length ratio between two elements, of which the diameters are different from each other, are shown in Figure 7. Obviously, the gyroscopic effect and bearing anisotropy in the rotor-bearing system cause separation of two natural frequencies. Since the proposed method, unlike the FEM, does not require re-meshing the system model every time the length ratio is changed, the aforementioned calculation can be readily performed along with varying only the element lengths of the model.

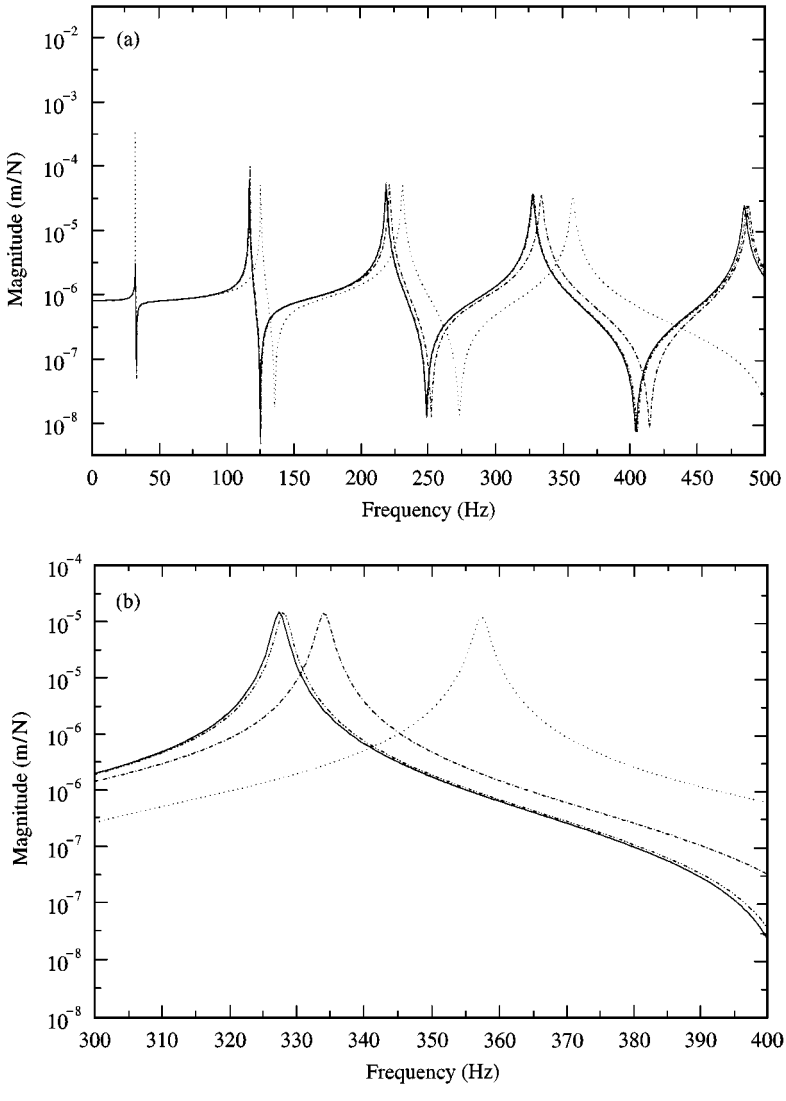

Figure 4. Driving point frequency response functions at node 1 for numerical model 1: (a) wide frequency range, (b) frequency region around the 4th mode. ———1 Element (proposed); - - - - 2 element (FEM); - · - · - 4 element (FEM) - ·· - ·· - 8 element (FEM).

3.3. NUMERICAL EXAMPLE 3

The present example deals with the multi-stepped rotor-bearing system exemplified in reference [6] in order to show the applicability of the proposed method to general rotor-bearing systems. Figure 8 is the cross-sectional drawing along the longitudinal axis of the shaft. The specifications of the rotor-bearing system are described in Table 3. In this case, 14 uniform elements are taken to model the multi-stepped shaft. Two different bearing sets are considered: one is

TABLE 1

Comparisons of eignevalues computed by the proposed method and the FEM (eigenvalues $\lambda_k = \sigma_k + j\omega_k$, rad/s)

	σ_k/ω_k			
Mode	FEM 4 elements	FEM 8 elements	FEM 12 elements	Proposed method 1 element
1st B*	−0·00746/206·54	−0·00746/206·49	−0·00746/206·49	−0·00746/206·49
1st F*	−0·00749/206·64	−0·00748/206·63	−0·00748/206·63	−0·00748/206·63
2nd B	−0·3912/741·10	−0·3867/738·83	−0·3864/738·70	−0·3863/738·65
2nd F	−0·3921/741·48	−0·3876/739·21	−0·3873/739·07	−0·3872/739·03
3rd B	−2·7273/1393·65	−2·6102/1379·17	−2·6034/1378·28	−2·6010/1377·97
3rd F	−2·7294/1394·25	−2·6123/1379·77	−2·6055/1378·88	−2·6032/1378·57

* B and F denote backward and forward modes respectively.

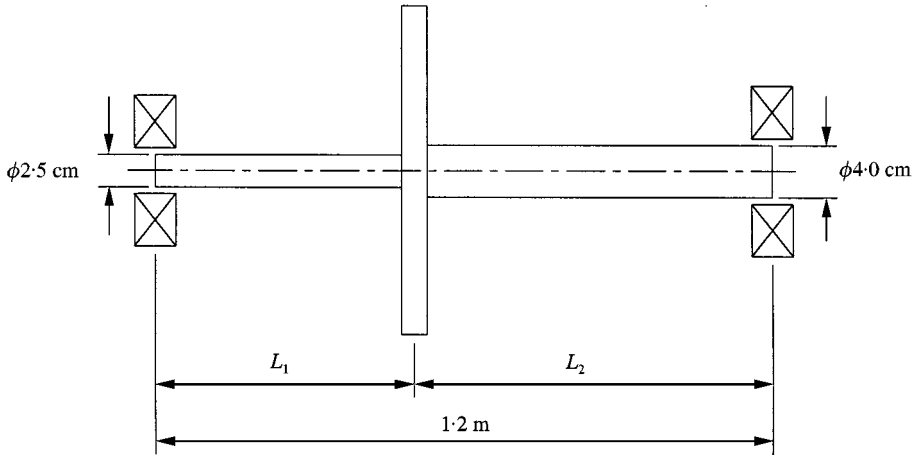

Figure 5. Numerical mode 2.

isotropic and the other is anisotropic. In Figure 9 are shown the unbalance responses at node 4 with the unbalance as described in Table 3. For the isotropic case, the whirl becomes a circle in that the minor and major whirl radii are identical. However, in the case of anisotropic bearings, the whirl becomes elliptic. The forward and backward critical speeds are clearly observed in this case.

TABLE 2

Specification of numerical model 2

Shaft	Length (m)		1·20
	Diameter (cm)		$d_1 = 2{\cdot}5$ $d_2 = 4$
	Young's modulus (GN/m^2)		200
	Density (kg/m^3)		8000
Disk	mass(kg)		20
	Polar moment of inertia ($kg\,m^2$)		0·163
	Diametral moment of inertia ($kg\,m^2$)		0·085
Bearing (2 identical)	Stiffness	k_{yy} (MN/m)	20
		k_{yz} (MN/m)	−1·5
		k_{zy} (MN/m)	−1·5
		k_{zz} (MN/m)	25
	Damping	c_{yy} (N s/m)	60
		c_{yz} (N s/m)	0
		c_{zy} (N s/m)	0
		c_{zz} (N s/m)	70

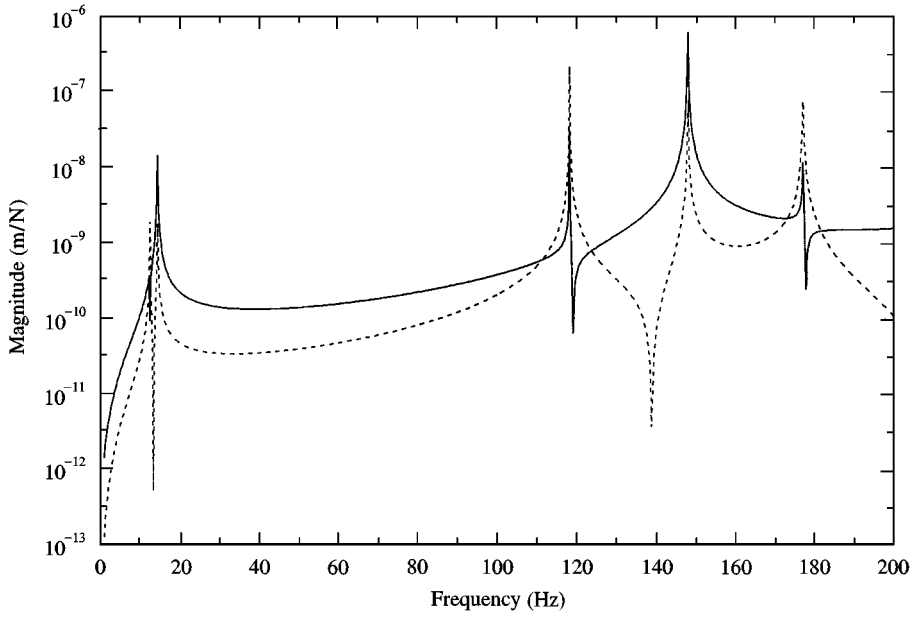

Figure 6. Typical FRFs measured and excited at nodes 1 and 3, respectively for numerical model 2 with $L_1/L_2 = 1{\cdot}0$. ——— forward; - - - - - backward.

4. CONCLUDING REMARKS

In this study, an exact dynamic matrix in Laplace domain for a Timoshenko shaft element is derived. The essence of the derivation procedure is to apply Laplace

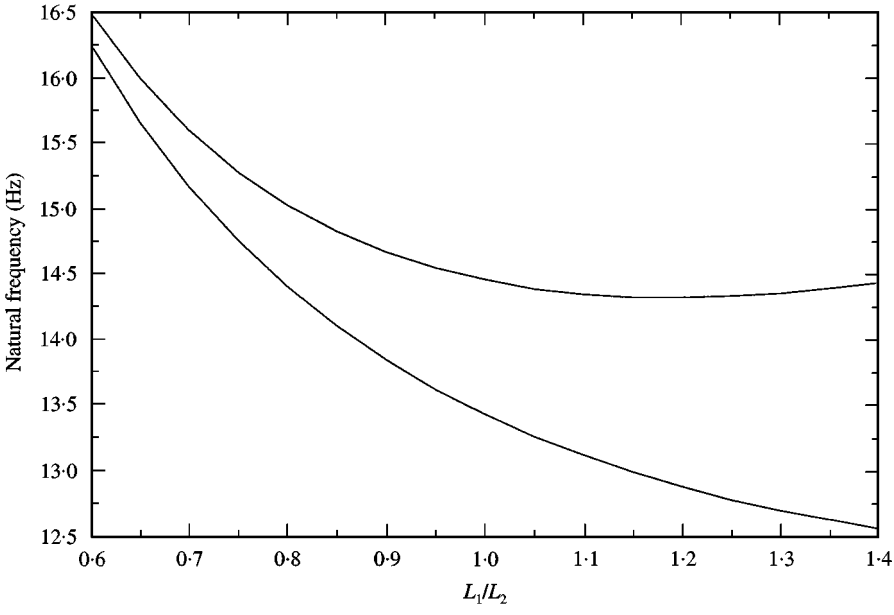

Figure 7. First two natural frequencies with L_1/L_2 varied for numerical model 2.

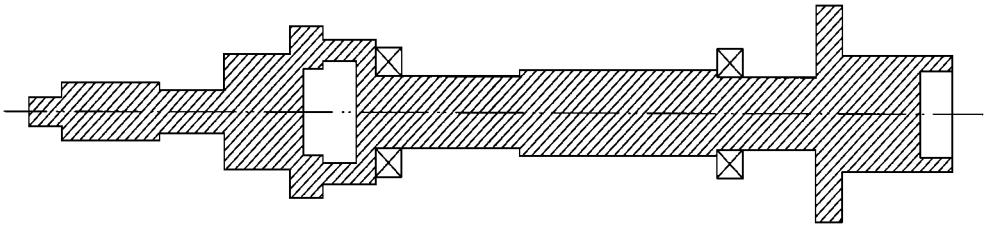

Figure 8. Numerical model 3.

transformation, twice with respect to time and also spatial co-ordinate, to a spatial state equation of the Timoshenko shaft model. Then inverse Laplace transformation of the resulting equation with respect to the spatial co-ordinate and application of the boundary values comes up with the exact dynamic matrix for a uniform shaft element. The exact dynamic matrix for the shaft element is used together with the other two element matrices for rigid disk and bearing so as to construct the global system dynamic matrix of a rotor-bearing system. Then, the dynamic analysis procedure to obtain eigensolutions, FRFs and unbalance responses is straightforward although the eigensolution analysis necessitates a special algorithm other than that for the conventional discrete system. Three

TABLE 3

Multi-stepped rotor configuration data for numerical model 3

Component	Element no.	Length (cm)	Outer radius (cm)	Inner radius (cm)
Shaft	1	1·27	0·51	0·0
	2	3·81	1·02	0·0
	3	2·54	0·76	0·0
	4	2·54	2·03	0·0
	5	0·51	3·03	0·0
	6	0·76	3·03	1·52
	7	1·27	2·54	1·78
	8	0·76	2·54	0·0
	9	5·59	1·27	0·0
	10	7·62	1·52	0·0
	11	3·81	1·27	0·0
	12	1·02	3·81	0·0
	13	3·04	2·03	0·0
	14	1·27	2·03	1·52

Disk	Node	Mass (kg)	Mass moment of intertia (kg m^2) Polar	Diametral
	4	1·401	0·0020	0·0136

	Node	c_{yy} (N s/m)	c_{yz} (N s/m)	c_{zy} (N s/m)	c_{zz} (N s/m)	Case
Bearing (2 identical)	9, 11	1752	0	0	1752	1
		1752	0	0	1752	2
		k_{yy} (N/m)	k_{yz} (N/m)	k_{zy} (N/m)	k_{zz} (N/m)	Case
		$4{\cdot}378 \times 10^7$	0	0	$4{\cdot}378 \times 10^7$	1
		$3{\cdot}503 \times 10^7$	$-8{\cdot}756 \times 10^6$	$-8{\cdot}756 \times 10^6$	$3{\cdot}503 \times 10^7$	2

Unbalance	Node	Magnitude (g mm)
	4	889·635

numerical examples are provided to show the adequacy and applicability of the proposed method.

The proposed method provides an exact model with finite matrix size for multi-stepped, distributed parameter rotor-bearing systems. Moreover, a drastic reduction in the size of the model is anticipated due to the fact that any uniform segment of the shaft can be modelled by one shaft element without causing any error. The proposed method also allows dynamic analysis of the system without any re-meshing process even in the case when shaft dimensions are changed. It is worthwhile to mention that the proposed method can be incorporated with the FEM for modelling and analysis of complicated systems.

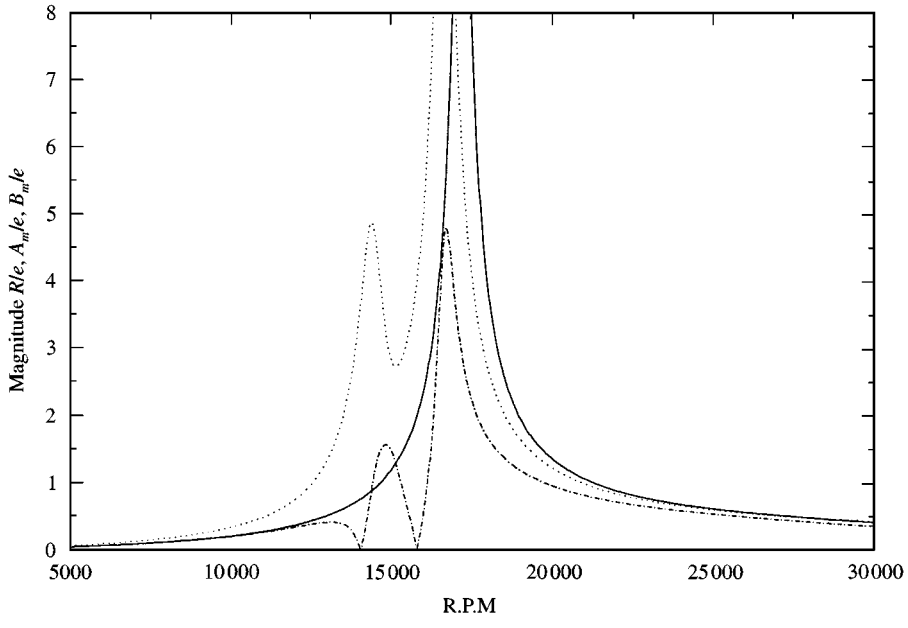

Figure 9. Unbalance response at node 4, normalized by eccentricity (e) for numerical model 3. —— Isotropic; ····· orthotropic (major), - - - - orthotropic (minor).

REFERENCES

1. J. W. Lund 1974 *ASME Journal of Engineering for Industry* **96**, 509–517. Stability and damped critical speeds of a flexible rotor in fluid film bearings.
2. J. S. Rao 1983 *Rotor Dynamics*. New York: Wiley.
3. N. F. Rieger 1971 *ASME Journal of Engineering for Power* **93**, 265–278. Unbalance response of an elastic rotor in damped flexible bearings at supercritical speeds.
4. R. L. Ruhl and J. F. Booker 1972 *ASME Journal of Engineering for Industry* **94**, 128–132. A finite element method for distributed parameter turbo-rotor systems.
5. R. Gasch 1972 *Journal of Sound and Vibration* **89**, 53–73. Vibration of large turbo rotors in fluid film bearings on elastic foundation.
6. H. D. Nelson and J. M. McVaugh 1976 *ASME Journal of Engineering for Industry* **98**, 593–600. The dynamics of rotor bearing systems using finite elements.
7. E. Hashish and T. S. Sanker 1984 *ASME Journal of Vibration, Acoustics, Stress and Reliability in Design* **106**, 80–898. Finite element and modal analyses of rotor bearing systems under stochastic loading conditions.
8. C. W. Lee and S. W. Hong 1990 *International Journal of Analytical and Experimental Modal Analysis*, **5**, 51–65. Asynchronous harmonic response analysis of rotor bearing systems.
9. S. W. Hong and J. H. Park 1997 *Journal of Sound and Vibration* **200**, 4891–504. An efficient method for the unbalance response analysis of rotor-bearing systems.
10. F. M. Dementberg 1961 *Flexural Vibrations of Rotating Shafts*. London: Butterworth.
11. C. W. Lee and Y. G. Jei 1988 *Journal of Sound and Vibration* **126**, 345–361. Modal analysis of continuous rotor bearing systems.
12. R. Catz, C. W. Lee, A. G. Ulsoy and R. A. Scott 1988 *Journal of Sound and Vibration* **122**, 119–130. The dynamics of a rotating shaft subject to a moving load.
13. C. W. Lee 1993 *Vibration Analysis of Rotors*. Dordrecht: Kluwer Academic Publishers.

14. B. YANG and H. FANG 1994 *Journal of Vibration and Acoustics* **116**, 426–432. Transfer function formulation of non-uniformly distributed parameter systems.
15. H. FANG and B. YANG 1998 *Journal of Sound and Vibration* **211**. Modelling, synthesis and dynamics analysis of complex flexible rotor systems.

APPENDIX A: EQUATIONS FOR A TIMOSHENKO SHAFT ELEMENT

$$[\lambda I - B]^{-1} = \frac{1}{(\lambda^2 - \alpha^2)(\lambda^2 - \beta^2)}$$

$$\times \begin{bmatrix} \lambda(\lambda^2 - ab) & \lambda^2 & -d\lambda^2 + b(ad+1) & b\lambda \\ -bc & \lambda(\lambda^2 - cd) & b\lambda & b(\lambda^2 - cd) \\ -c(\lambda^2 - ab) & -c\lambda & \lambda(\lambda^2 - cd) & -bc \\ -c\lambda & a\lambda^2 - c(ad+1) & \lambda^2 & \lambda(\lambda^2 - cd) \end{bmatrix}, \tag{A1}$$

$$\alpha^2 = \tfrac{1}{2}\{(ab+cd) + \sqrt{(ab+cd)^2 - 4(abcd+bc)}\},$$

$$\beta^2 = \tfrac{1}{2}\{(ab+cd) - \sqrt{(ab+cd)^2 - 4(abcd+bc)}\}, \tag{A2}$$

$$C(x,s) = \begin{bmatrix} f_3 - abf_1 & f_2 & -df_2 + (abd+b)f_b & bf_1 \\ -bcf_0 & f_3 - cdf_1 & bf_1 & bf_2 - bcdf_0 \\ -cf_2 + abcf_0 & -cf_1 & f_3 - abf_1 & -bcf_0 \\ -cf_1 & af_2 - (acd+c)f_0 & f_2 & f_3 - cdf_1 \end{bmatrix}, \tag{A3}$$

$$f_0 = L^{-1}\left(\frac{1}{(\lambda^2 - \alpha^2)(\lambda^2 - \beta^2)}\right) = \frac{1}{\alpha^2 - \beta^2}\left(\frac{1}{\alpha}\sinh \alpha x - \frac{1}{\beta}\sinh \beta x\right).$$

$$f = L^{-1}\left(\frac{\lambda}{(\lambda^2 - \alpha^2)(\lambda^2 - \beta^2)}\right) = \frac{1}{\alpha^2 - \beta^2}(\cosh \alpha x - \cosh \beta x),$$

$$f_2 = L^{-1}\left(\frac{\lambda}{(\lambda^2 - \alpha^2)(\lambda^2 - \beta^2)}\right) = \frac{1}{\alpha^2 - \beta^2}(\alpha \sinh \alpha x - \beta \sinh \beta x),$$

$$f_3 = L^{-1}\left(\frac{\lambda^3}{(\lambda^2 - \alpha^2)(\lambda^2 - \beta^2)}\right) = \frac{1}{\alpha^2 - \beta^2}(\alpha^2 \cosh \alpha x - \beta^2 \cosh \beta x), \tag{A4}$$

$$\Delta = 2b(1 - \cosh \alpha l \cosh \beta l) + \frac{\alpha\beta}{c}\{\zeta^2 + \eta^2\}\sinh \alpha l \sinh \beta l,$$

$$d_1 = -\zeta \sinh \alpha l \cosh \beta l + \eta \sinh \beta l \cosh \alpha l,$$

$$d_2 = \frac{(\beta\zeta + \alpha\eta)}{\alpha^2 - \beta^2} \sinh \alpha l \sinh \beta l - \frac{(ab - cd)}{\alpha^2 - \beta^2} (1 - \cosh \alpha l \cosh \beta l),$$

$$d_3 = \frac{\alpha\beta}{bc} \{\eta \sinh \alpha l \cosh \beta l - \zeta \sinh \beta l \cosh \alpha l\},$$

$$d_4 = \zeta \sinh \alpha l - \eta \sinh \beta l,$$

$$d_5 = \cosh \alpha l - \cosh \beta l,$$

$$d_6 = \frac{\alpha\beta}{bc} \{-\eta \sinh \alpha l + \zeta \sinh \beta l\}.$$

$$\zeta = \frac{(cd - \alpha^2)}{\alpha}, \quad \eta = \frac{(cd - \beta^2)}{\beta}, \tag{A5}$$

$$\hat{\Delta} = 2b(1 - \cosh \hat{\alpha} l \cosh \hat{\beta} l) + \frac{\hat{\alpha}\hat{\beta}}{c} \{\hat{\zeta}^2 + \hat{\eta}^2\} \sinh \hat{\alpha} l \sinh \hat{\beta} l,$$

$$\hat{d}_1 = -\hat{\zeta} \sinh \hat{\alpha} l \cosh \hat{\beta} l + \hat{\eta} \sinh \hat{\beta} l \cosh \hat{\alpha} l,$$

$$\hat{d}_2 = \frac{(\hat{\beta}\hat{\zeta} + \hat{\alpha}\hat{\eta})}{\hat{\alpha}^2 - \hat{\beta}^2} \sinh \hat{\alpha} l \sinh \hat{\beta} l - \frac{(\hat{a}b - cd)}{\hat{\alpha}^2 - \hat{\beta}^2} (1 - \cosh \hat{\alpha} l \cosh \hat{\beta} l),$$

$$\hat{d}_3 = \frac{\hat{\alpha}\hat{\beta}}{bc} \{\hat{\eta} \sinh \hat{\alpha} l \cosh \hat{\beta} l - \hat{\zeta} \sinh \hat{\beta} l \cosh \hat{\alpha} l\},$$

$$\hat{d}_4 = \hat{\zeta} \sinh \hat{\alpha} l - \hat{\eta} \sinh \hat{\beta} l,$$

$$\hat{d}_5 = \cosh \hat{\alpha} l - \cosh \hat{\beta} l,$$

$$\hat{d}_6 = \frac{\hat{\alpha}\hat{\beta}}{bc} \{-\hat{\eta} \sinh \hat{\alpha} l + \hat{\zeta} \sinh \hat{\beta} l\}.$$

$$\hat{\zeta} = \frac{(cd - \hat{\alpha}^2)}{\hat{\alpha}}, \quad \hat{\eta} = \frac{(cd - \hat{\beta}^2)}{\hat{\beta}}, \tag{A6}$$

$$\hat{\alpha}^2 = \tfrac{1}{2}\{(\hat{a}b + cd) + \sqrt{(\hat{a}b + cd)^2 - 4(\hat{a}bcd + bc)}\},$$

$$\hat{\beta}^2 = \tfrac{1}{2}\{(\hat{a}b + cd) - \sqrt{(\hat{a}b + cd)^2 - 4(\hat{a}bcd + bc)}\}, \tag{A7}$$